

Electronic density of states and bonding in chalcopyrite-type semiconductors*

Carmen Varea de Alvarez[†] and Marvin L. Cohen[†]

Department of Physics and I.M.R.D., Lawrence Berkeley Laboratory, University of California, Berkeley, California 94720

L. Ley, S. P. Kowalczyk, F. R. McFeely, and D. A. Shirley

Department of Chemistry and Lawrence Berkeley Laboratory, University of California, Berkeley, California 94720

R. W. Grant

Science Center, Rockwell International, Thousand Oaks, California 91360

(Received 14 December 1973)

Measured x-ray-photoemission spectra for ZnGeP₂ and CdSnAs₂ are presented along with density-of-states $N(E)$ and charge-density calculations for ZnGeP₂. Analysis of the density-of-states spectra illustrates the relation between $N(E)$ structure and bonding properties, allowing spectral peaks to be assigned to specific bonds.

We have calculated the valence-band density of states $N(E)$ and measured the x-ray-photoemission (XPS) spectrum $I(E)$ for the chalcopyrite-type semiconductor ZnGeP₂. $I(E)$ was also measured for CdSnAs₂. In ZnGeP₂ the shapes of $N(E)$ and $I(E)$ agreed very well, allowing us to correlate structure in $I(E)$ explicitly with Zn-P and Ge-P bonds through contour plots of electron charge densities integrated over selected *energy* intervals $\rho_{\Delta E}(\vec{r})$. This approach appears promising for a detailed understanding of bonding in chalcopyrite-type compounds and other ternary or more complex materials.

The $A^{II}B^{IV}C_2^V$ compounds are ternary analogs of the $B^{III}C^V$ zinc-blende semiconductors (e.g., ZnGeP₂ is the analog of GaP) in which alternate cation sites are occupied by atoms of the group-II and group-IV elements surrounded in tetrahedral coordination by group-V anions. The ternary compounds, therefore, possess an essential complication that is absent in their binary analogs—two kinds of bonds. The present work represents the first attempt to relate features in $N(E)$ or $I(E)$ to different bonds in a relatively complex material, thereby extending a correlation that is obvious for the diamond and zinc-blende lattices.^{1,2}

Our approach was to compute the charge density $\rho_{\Delta E}(\vec{r})$ within an energy region ΔE rather than the usual $\rho_n(\vec{r})$, the charge density for band n . The energy region was chosen to correspond to an energy interval in which $N(E)$ contains structure of interest (e.g., a peak). For ZnGeP₂ there appears to be six important regions in $N(E)$. These are labeled *A*, *B*, *C*, *D*, *E*, and *F* in Fig. 1. Figure 2 shows $\rho_{\Delta E}(\vec{r})$ for each region, calculated in the $x=y$ plane, which contains the Zn, Ge, and P ions. The experimental results will be described next, followed by a discussion of the calculation and an analysis of the results.

Single crystals of ZnGeP₂ and CdSnAs₂ were

grown by directional solidification of stoichiometric melts synthesized from the elements. The photoelectron spectra were measured in a Hewlett-Packard 5950 ESCA Spectrometer (which uses monochromatized Al K_{α} x rays) modified to operate at pressures well below 10^{-9} Torr. Samples of the single crystals were fractured inside the spectrometer immediately before the measurements. The freshly exposed surfaces showed no detectable oxygen or carbon contamination even after 12 h. Valence-band spectra $I(E)$ referred to the top of the valence band are shown in Fig. 1. These spectra have been corrected for contributions from inelastically scattered electrons.³ The intense peaks corresponding to emission of core-like Zn 3*d* and Cd 4*d* electrons have been truncated to exhibit the valence *s* and *p* contributions more clearly. The unperturbed shape of the *d* peaks is indicated by solid curves in Fig. 1.

We first give a brief description of the spectrum, which we will analyze in detail later. Starting at the top of the valence band, $I(E)$ rises in both compounds to an intense, broad peak at a binding energy of 2–4 eV. This peak exhibits a wealth of fine structure. After a well-defined minimum at 6.2 eV in ZnGeP₂ and 5.7 eV in CdSnAs₂, the intensity rises again. In CdSnAs₂ a blunt hump is observed around 7.0 eV, with a satellite at 8.3 eV. Beyond 8.5 eV $I(E)$ follows closely the sharp onset of the leading edge of the 4*d* peak. Valence-band contributions to $I(E)$ cannot be distinguished at higher binding energies.

In ZnGeP₂ a second region of high-valence electron density can be identified around 7.0 eV on the leading edge of the Zn 3*d* peak. A drop in intensity of peak II beyond 8.0 eV seems likely, but is not certain. There is a shoulder on the low-energy (high-binding-energy) side of the Zn 3*d* peak that cannot be explained by oxidation, plasmon losses, multiplet splitting, or shakeup processes. We

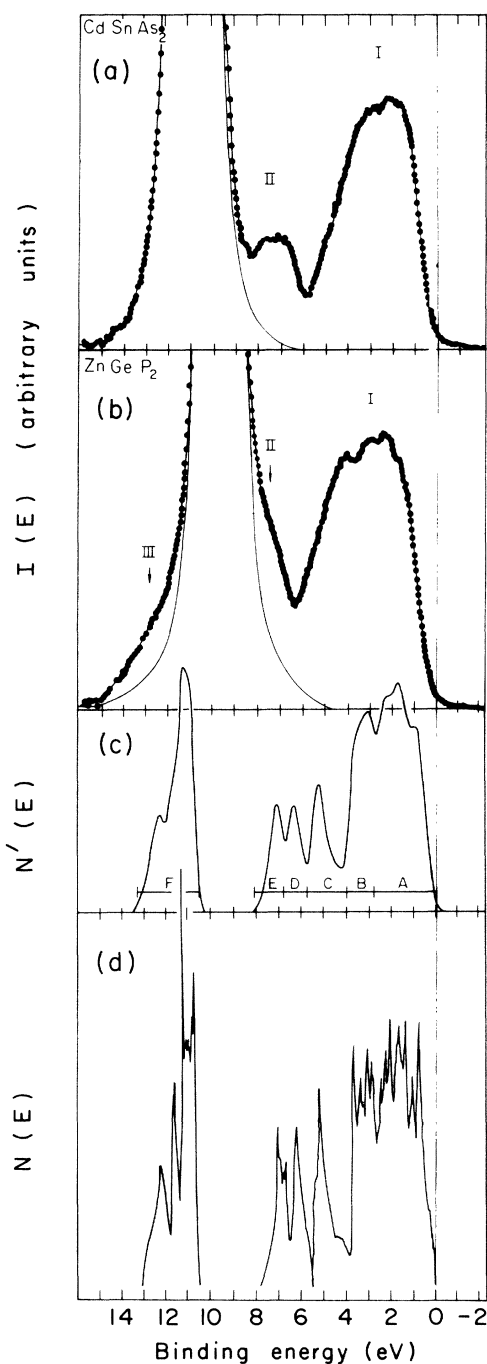


FIG. 1. (a) XPS spectrum for CdSnAs_2 ; (b) spectrum for ZnGeP_2 ; (c) broadened theoretical density of states for ZnGeP_2 ; (d) calculated valence-band density of states for ZnGeP_2 .

therefore interpret that shoulder as due to a third valence-band peak centered at ~ 12.5 eV, with a total width of about 4 eV at its base. This determines the total valence bandwidth in ZnGeP_2 as 14.5 ± 0.5 eV. A corresponding third peak in CdSnAs_2 is presumably masked by the Cd $4d$ peak.

Its position is then limited to a range of between 10.0 and 12.5 eV.

The band-structure calculations for ZnGeP_2 were based on the empirical pseudopotential method.⁴ No attempt was made to fit the pseudopotential to experiment. The method of choosing the potential and the resulting band structure is given in Ref. 5.

In analyzing the band structure, it is helpful to use the quasicubic model.⁶ In this model, the band structure of the chalcopyrite semiconductor is viewed as a perturbed version of its zinc-blende analog. In a typical zinc-blende semiconductor, $N(E)$ exhibits the following prominent structure¹: a broad peak (peak I) near the top of the valence band, separated from a second narrower peak (peak II) by a small valley, followed by a gap which separates this structure from the lowest energy peak III. Charge-density calculations² for each of the valence bands separately give some indication of the electron distribution in the zinc-blende case. States in peak I correspond to electrons near the

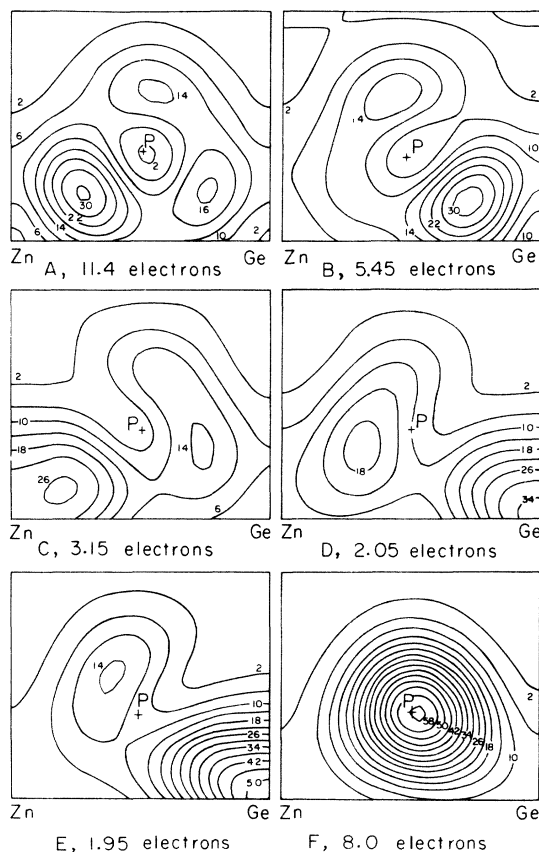


FIG. 2. Calculated electronic charge-density contour plots for ZnGeP_2 corresponding to density-of-states peaks A, B, C, D, E, and F. The plots are normalized to the number of electrons contained in each peak. This value is given for each plot.

bonding sites, peak II contains electrons which are mostly *s*-like around the cation and some charge piled up in the bonding region, and peak III contains electrons which are *s*-like around the anion.

In the chalcopyrites one expects that the overall $N(E)$ should be similar, but that more structure should be present. For example, peak I should contain structure arising from the two types of bonds. Since this calculation was based on a local pseudopotential, one expects the same problems that were encountered with local pseudopotentials for the zinc blendes.² In particular, a nonlocal scheme^{2,4} was necessary to obtain the correct width of peak I in the zinc blendes. The local potential gives a peak I that is too narrow. We therefore expect the peak-I region to be too narrow in the chalcopyrite case; however, the basic features of the structure should not be affected.

Figure 1 contains the results for the calculated $N(E)$ for ZnGeP_2 and the measured XPS spectra for ZnGeP_2 and CdSnAs_2 . Critical points in the band structure show up as sharp structure in $N(E)$. To facilitate comparison with experiment, a Gaussian-broadened curve $N'(E)$ is also shown. Figure 2 shows $\rho_{\Delta E}(\vec{r})$. The energy intervals ΔE were chosen through analysis of $N'(E)$; $\rho_{\Delta E}(\vec{r})$ was then calculated for each interval by restricting the band indices and k states to give electron states in the desired energy range ΔE .

Referring to Fig. 1, we see that the highest-energy (lowest-binding-energy) valence-band structure, which corresponds to peak I in the zinc-blende case, is split into two regions, *A* and *B*. Using the $\rho_A(\vec{r})$ and $\rho_B(\vec{r})$ of Fig. 2, we see that these regions contain electrons in the Zn-P and Ge-P bonds, respectively. The number of electrons in the energy interval *A* is 11.4 and there are 5.45 electrons in the *B* region. Peak I is therefore split by the energy difference in the two bonds. The Ge-P bond appears to be a stronger covalent bond (i. e., it lies lower in energy) than the Zn-P bond, as would be expected on chemical grounds. The theoretical width of peak I is smaller than experiment; this could arise either from the use of the local potential as described before, or from an underestimation of the difference between the potentials of the two cations. The general shape

and splitting of peak I, however, shows excellent agreement between the experimental and theoretical spectra, with four distinct corresponding features present in each.

The peak-II region splits into three peaks *C*, *D*, and *E*. In the binary semiconductors, $\rho(\vec{r})$ shows some concentration around the cation with some charge in the bond. For ZnGeP_2 in the *C* region (3.15 electrons), charge concentrates on Zn with some charge in the Ge-P bond, while region *D* (2.05 electrons) and *E* (1.95 electrons) show charge accumulating on Ge. This order is expected because the Ge potential is deeper than that of Zn. In region *D* there is some charge in the Zn-P bond, while *E* shows some charge piled up in the anti-bonding region. In the XPS spectra, peak II is partially hidden by the *d* peaks. In CdSnAs_2 , by measuring the relative areas under the experimental spectrum and comparing this with the theoretical curve of ZnGeP_2 , we conclude that the structure in the region between 6.5 and 7.5 eV probably corresponds to the *D* and *C* unresolved doublet. The satellite at 8.3 eV is interpreted as arising from region *E*. It is unfortunate that the peak-II region is not easier to discern, as this region is most affected by the differences in the cation potentials.

As discussed before, peak III is observed in the ZnGeP_2 XPS spectrum, but hidden in the CdSnAs_2 spectrum. In the theoretical $N'(E)$ this region is labeled *F*. There are eight electrons in this region and $\rho_F(\vec{r})$ shows that the electrons are mostly *s* like around the anion, i. e., the *P* site. This is the same configuration found in zinc-blende-type semiconductors, as is expected, as the phosphorous 3s subshell is tightly enough bound to be nearly corelike.

The above analysis illustrates the advantages of dealing with both $\rho_{\Delta E}(\vec{r})$ and $N(E)$. We have concentrated on ZnGeP_2 in this work, but the results should be general for the chalcopyrite-type compounds. The possibility of identifying certain features in $I(E)$ with well-defined charge distributions and specific bonds should be especially useful in the analysis of complex or amorphous materials, which as yet defy a realistic theoretical treatment.

We thank H. Nadler of the Science Center, Rockwell International, for growing the ZnGeP_2 crystal.

*Work performed under the auspices of the U. S. Atomic Energy Commission.

†Supported in part by National Science Foundation Grant No. GP 35688.

¹L. Ley, S. Kowalczyk, R. Pollak, and D. A. Shirley, Phys. Rev. Lett. **29**, 1088 (1972); R. A. Pollak, L. Ley, S. Kowalczyk, D. A. Shirley, J. D. Joannopoulos D. J. Chadi, and M. L. Cohen, *ibid.* **29**, 1103 (1972).

²J. Chelikowsky, D. J. Chadi, and M. L. Cohen, Phys. Rev. B **8**, 2786 (1973); J. P. Walter and M. L. Cohen, *ibid.* **4**, 1877 (1971).

³R. G. Cavell, S. P. Kowalczyk, L. Ley, R. A. Pollak, B. Mills, D. A. Shirley, and W. Perry, Phys. Rev. B **7**, 5313 (1973).

⁴M. L. Cohen and V. Heine, Solid State Phys. **24**, 37 (1970).

⁵C. Varea de Alvarez and M. L. Cohen, Phys. Rev. Lett. **30**, 979 (1973).

⁶For example, J. E. Rowe and J. L. Shay, Phys. Rev. **3**, 451 (1971), and references given in Ref. 5 of the present paper. References to earlier experimental work are also given in Ref. 5.